Chemical Denaturation of the Elongation Factor 1α Isolated from the Hyperthermophilic Archaeon *Sulfolobus solfataricus*†

Vincenzo Granata,‡ Giuseppe Graziano,§ Alessia Ruggiero,‡ Gennaro Raimo,||,⊥ Mariorosario Masullo,⊥,# Paolo Arcari,⊥ Luigi Vitagliano,¶,£ and Adriana Zagari*,‡,¶

Dipartimento delle Scienze Biologiche, Sezione di Biostrutture, Università degli Studi di Napoli Federico II, I-80134 Napoli, Italy, Dipartimento di Scienze Biologiche ed Ambientali, Università del Sannio, I-82100 Benevento, Italy, Dipartimento di Scienze e Tecnologie per l'Ambiente e il Territorio, Università degli Studi del Molise, I- 86170 Isernia, Italy, Dipartimento di Biochimica e Biotecnologie Mediche, Università degli Studi di Napoli Federico II, I-80131 Napoli, Italy, Dipartimento di Scienze Farmacobiologiche, Università degli Studi "Magna Graecia" di Catanzaro, Roccelletta di Borgia, I-88021 Catanzaro, Italy, Istituto di Biostrutture e Bioimmagini, CNR, I-80134 Napoli, Italy, and Centro Interuniversitario di Ricerca sui Peptidi Bioattivi (CIRPEB), I-80134 Napoli, Italy

Received March 15, 2005; Revised Manuscript Received November 22, 2005

ABSTRACT: The stability against chemical denaturants of the elongation factor EF-1α (*Ss*EF-1α), a protein isolated from the hyperthermophilic archaeon *Sulfolobus solfataricus* has been characterized in detail. Indeed, the atypical shape of the protein structure and the unusual living conditions of the host organism prompted us to analyze the effect of urea and guanidine hydrochloride (GuHCl) on the GDP complex of the enzyme (*Ss*EF-1α·GDP) by fluorescence and circular dichroism. These studies were also extended to the nucleotide-free form of the protein (nf*Ss*EF-1α). Interestingly, the experiments show that the denaturation curves of both *Ss*EF-1α forms present a single inflection point, which is indicative of a cooperative unfolding process with no intermediate species. Moreover, the chemically induced unfolding process of both *Ss*EF-1α·GDP and nf*Ss*EF-1α is fully reversible. Both *Ss*EF-1α forms exhibit remarkable stability against urea, but they do not display a strong resistance to the denaturing action of GuHCl. These findings suggest that electrostatic interactions significantly contribute to *Ss*EF-1α stability.

The elongation factors (EFs)[1] that catalyze the binding of the aminoacyl-tRNA to the ribosome are ubiquitous and highly conserved guanine nucleotide-binding proteins (GNBP) (*1*, *2*). They consist of a single polypeptide chain with a length of 390−460 residues. In performing their biological functions, these EFs interact with several cellular components: GDP, GTP, Mg^{2+}, aminoacyl-tRNA, exchange factors, and ribosome (*1*, *3*−*6*).

The comparison of EF sequences derived from organisms of the three living domains shows that archaeal EFs are more similar to eukaryal EFs than to eubacterial EFs. Indeed, eubacterial factors, denoted as EF-Tu, display sequence identities that fall in the 30−40% range when compared to archaeal EFs (*7*). On the other hand, the sequences of archaeal and eukaryal EFs, collectively designated EF-1α, share sequence identities in the 50−60% range (*7*).

From the structural point of view, the extensively characterized EF-Tu shows intriguing properties (*3*). Indeed, the interactions with both small and large ligands produce large rearrangements of the enzyme structure (*5*, *6*, *8*−*12*). Particularly impressive is the interdomain reorganization observed between the active GTP-bound and the inactive GDP-bound forms (*5*, *6*). Large variations also occur upon the interaction of EF-Tu with the exchange factor (*11*, *12*) and with antibiotics (*10*).

Although only limited structural information is available for EF-1α, the first crystallographic investigations have provided insight into differences and analogies between EF-Tu and EF-1α (*13*−*15*). As for EF-Tu, the GDP complex of *Sulfolobus solfataricus* EF-1α (*Ss*EF-1α) shows an open structure with few interdomain interactions (*15*). On the other hand, the association between *Saccharomyces cerevisiae* EF-1α (*Sc*EF-1α) and its nucleotide exchange factor is completely different from that observed in the EF-Tu enzymes (*13*). Nevertheless, the comparison of *Ss*EF-1α and *Sc*EF-1α shows that the enzyme function relies on a large structural flexibility as found in its eubacterial counterpart (*15*).

In the present paper, we report a characterization of the stability against chemical denaturants of *Ss*EF-1α, a protein isolated from a hyperthermophilic archaeon (*16*). The chemi-

† This work was supported by MIUR, PRIN 2003.

* To whom correspondence should be addressed: Dipartimento delle Scienze Biologiche, Sezione di Biostrutture, Università degli Studi di Napoli Federico II, Via Mezzocannone 16, I-80134 Napoli, Italy. E-mail: zagari@unina.it. Telephone: +39-081-2536613. Fax: +39-081-2536603.

‡ Dipartimento delle Scienze Biologiche, Università degli Studi di Napoli Federico II.

§ Università del Sannio.

|| Università degli Studi del Molise.

⊥ Dipartimento di Biochimica e Biotecnologie Mediche, Università degli Studi di Napoli Federico II.

Università degli Studi "Magna Graecia".

¶ Istituto di Biostrutture e Bioimmagini, CNR.

£ Centro Interuniversitario di Ricerca sui Peptidi Bioattivi.

[1] Abbreviations: GNBP, guanine nucleotide-binding proteins; EF, elongation factor; *Sc*EF-1α, EF-1α isolated from *Saccharomyces cerevisiae*; *Ss*EF-1α, EF-1α isolated from *Sulfolobus solfataricus*; nf*Ss*EF-1α, nucleotide-free *Ss*EF-1α; *Ss*EF-1α·GDP, complex of *Ss*EF-1α with GDP; GuHCl, guanidine hydrochloride; CD, circular dichroism.

10.1021/bi050479d CCC: $33.50
Published on Web 12/24/2005

cal denaturation of the GDP complex of the enzyme was investigated by circular dichroism (CD) and fluorescence. Notably, these experiments demonstrate that *Ss*EF-1α·GDP unfolds in a reversible and cooperative manner, despite the peculiar shape of the complex, which is stabilized by few interdomain contacts (*15*). In addition, we report the preparation and the characterization of the nucleotide-free form of this enzyme (nf*Ss*EF-1α), which also exhibits a reversible and cooperative unfolding. These findings have been interpreted using the structural data available on the enzyme.

EXPERIMENTAL PROCEDURES

Preparation of SsEF-1α and Its Nucleotide-Free Form. Recombinant *Ss*EF-1α was prepared by using an *Escherichia coli* expression system following the procedure described previously (*17*). The protein was stored at −20 °C in a buffer containing 20 mM Tris/HCl (pH 7.8), 50 mM KCl, 10 mM $MgCl_2$, and 50% (v/v) glycerol.

The ligand-free form of the enzyme (nf*Ss*EF-1α) was prepared from the recombinant *Ss*EF-1α by adopting the procedure reported by Raimo et al. (*18*) that was based on the method initially developed for the small GNBP H-ras (*19*). The functionality of nf*Ss*EF-1α has been checked by measuring both the intrinsic GTPase activity and the GDP-binding ability of the enzyme (*16*). These experiments showed that the enzyme was fully active, even after a storage for several weeks at 4 °C (data not shown).

CD and Fluorescence Spectra. All CD spectra were recorded with a Jasco J-810 spectropolarimeter equipped with a Peltier temperature control system (Model PTC-423-S). The spectropolarimeter was calibrated with an aqueous solution of 1S-(+)-10-camphorsulfonic acid at 290 nm. Molar ellipticity per mean residue, $[\theta]$ in degrees cm^2 $dmol^{-1}$, was calculated from the equation: $[\theta] = [\theta]_{obs}mrw(10lC)^{-1}$, where $[\theta]_{obs}$ is the ellipticity measured in degrees, mrw is the mean residue molecular mass (111.5 Da), C is the protein concentration in g L^{-1}, and l is the optical path length of the cell in centimeters. Far-UV measurements (183−250 nm) were carried out at 20 °C using a 0.01 cm optical path-length cell and a protein concentration of 3.0 mg mL^{-1}. Near-UV spectra (250−320 nm) were collected at 20 °C using a 0.5 cm path-length cell and a protein concentration of 3.0 mg mL^{-1}. CD spectra, recorded with a time constant of 4 s, a 2 nm bandwidth, and a scan rate of 5 nm min^{-1}, were signal-averaged over at least three scans. The baseline was corrected by subtracting the buffer spectrum.

Fluorescence spectra were collected at 20 °C using a Varian Cary Eclipse spectrofluorimeter and a 1.0 cm path-length cell. Two separate sets of experiments were carried out, setting the excitation wavelength at either 280 or 295 nm. In both cases, the excitation and the emission slit widths were 5 nm.

Chemical Denaturation Experiments. A buffer solution containing 10 mM of sodium phosphate (pH 7.0) was used in all of the chemical denaturation experiments. Chemical denaturants urea and guanidine hydrochloride (GuHCl) were purchased from Sigma. Urea was further purified by recrystallization from ethanol/water (1:1) mixtures and used immediately after preparation. A commercial 8 M GuHCl solution was utilized. Stock solutions of urea and GuHCl, in different amounts, were mixed with protein solutions to give a constant final value of the protein concentration (0.15 mg mL^{-1}). The final concentration of urea and GuHCl was in the range of 0.0−9.6 and 0.0−7.0 M, respectively. The final pH for each sample was corrected by adding concentrated solutions of HCl or NaOH because high concentrations of urea and GuHCl affect the pH of the solution. Each sample was incubated overnight. Longer incubation times led to identical spectroscopic signals.

The urea- and GuHCl-induced denaturations were investigated by recording the CD signal at 222 nm, and the intensity change of the fluorescence signal at a fixed wavelength. The reversibility of the unfolding process has been initially proved by checking the optical properties of nfSsEF-1α and SsEF-1α·GDP after the removal of the denaturing agents by ultrafiltration. Furthermore, the reversibility was also checked by recording a CD renaturation curve (at 222 nm) upon a stepwise dilution of a protein solution from 5 to 0.5 M GuHCl. The functionality of the diluted solution containing 0.5 M GuHCl was also tested. In particular, the GDP-binding ability and the GTPase activity of the enzyme were analyzed following the procedure reported by Masullo et al. (*16*) (see also the Supporting Information).

RESULTS

Spectroscopic Characterization of nfSsEF-1α and SsEF-1α·GDP. CD spectra of nf*Ss*EF-1α and *Ss*EF-1α·GDP were recorded at 20 °C in both the far-UV and the near-UV regions. The far-UV CD spectra of *Ss*EF-1α·GDP (Figure 1A) and nf*Ss*EF-1α (Figure 1B) are practically identical. The maximum centered at 195 nm and the broad minimum centered at 222 nm are indicative of the presence of both α and β secondary-structure elements. A quantitative estimation of the secondary-structure content, performed by using the self-consistent method (*20*) implemented in DICHROWEB (*21*), showed that the α helix, the β sheet, and the unordered region contents are 29, 40, and 31%, respectively. These values are in line with those derived from the X-ray structure of *Ss*EF-1α complexed with GDP (*15*, *22*) and those estimated by FT-IR measurements (*23*). The near-UV CD spectra of nf*Ss*EF-1α and *Ss*EF-1α·GDP (Figure 2) are similar with positive and negative extrema located at identical wavelengths, even though their intensities are slightly different. This finding indicates that aromatic side chains of the protein have similar microenvironments in either the absence or presence of GDP. These data confirm the integrity of the folded structure of *Ss*EF-1α even after the removal of GDP.

The far-UV CD spectra of both *Ss*EF-1α forms either at 9.6 M urea or 7.0 M GuHCl are also shown in parts A and B of Figure 1. It is evident that at a high concentration of GuHCl the molar ellipticity of *Ss*EF-1α is close to 0. This is an indication that the unfolded state produced by GuHCl does not contain residual secondary structure. On the other hand, a significant CD signal is still detectable at high concentrations of urea. This suggests that urea leads to an unfolded state of the protein, which still contains a significant amount of secondary structure.

The steady-state fluorescence properties of *Ss*EF-1α·GDP and nf*Ss*EF-1α were studied using both 280 and 295 nm

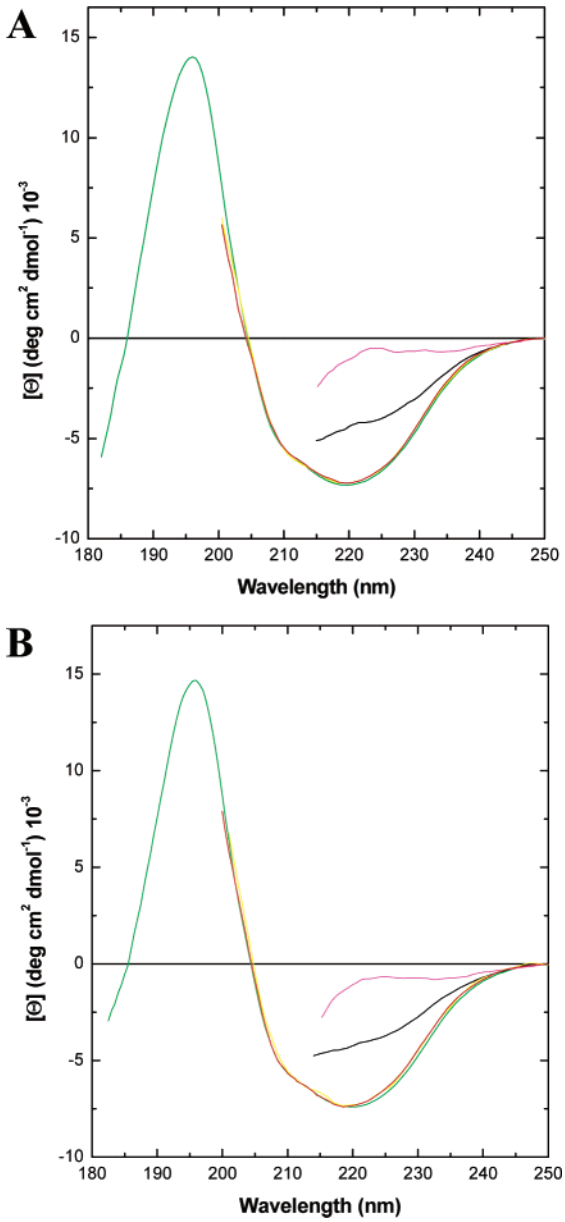

FIGURE 1: Far-UV CD spectra of *Ss*EF-1α·GDP (A) and nf*Ss*EF-1α (B). The spectra of the native proteins (green) and of the denatured forms, which were obtained with either urea (black) or GuHCl (magenta), were recorded at 20 °C in 10 mM phosphate buffer (pH 7.0). Denaturations were achieved by incubating overnight the protein solution with 9.6 M urea or 7 M GuHCl. Because of the absorption of urea and GuHCl molecules, the spectra of the denaturated proteins could only be registered from 250 to 215 nm. The spectra of the refolded species obtained after the removal of urea (yellow) and GuHCl (red), which are virtually identical to those of the native proteins, are also shown (wavelength interval of 200−250 nm).

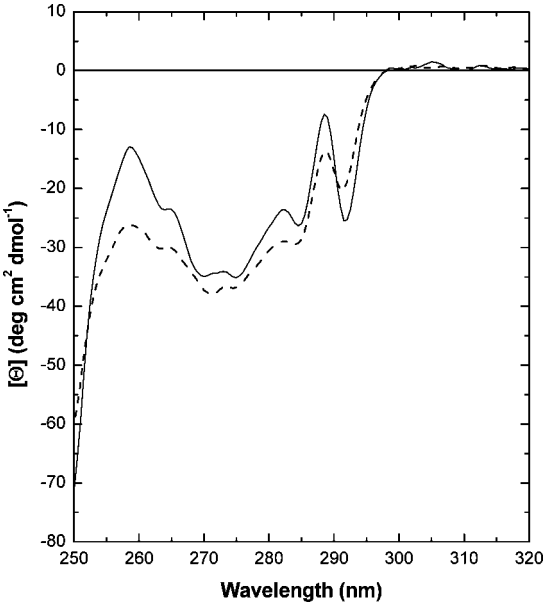

FIGURE 2: Near-UV CD spectra of nf*Ss*EF-1α (—) and *Ss*EF-1α·GDP (- - -). The spectra were recorded at 20 °C in 10 mM phosphate buffer (pH 7.0).

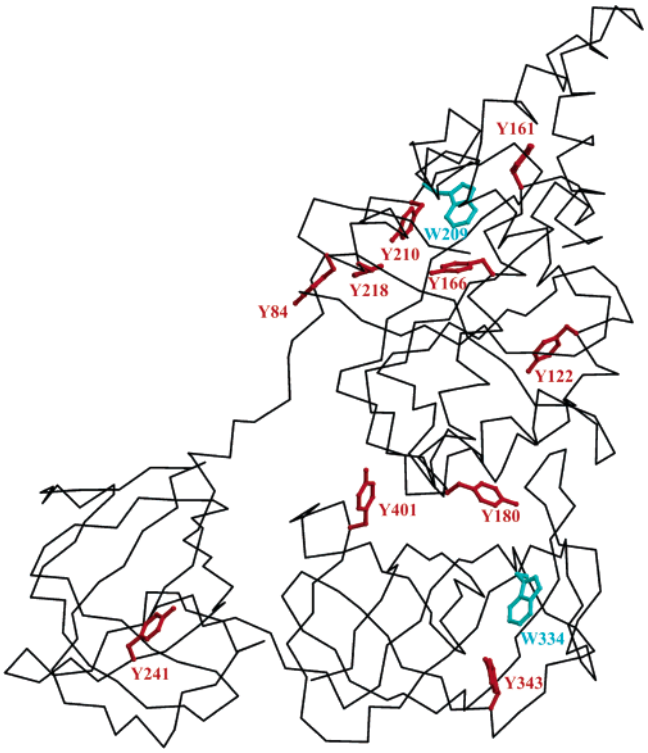

FIGURE 3: Location of Tyr (red) and Trp (cyan) residues in the *Ss*EF-1α·GDP structure. The figure was generated using MOLSCRIPT (*42*) and RASTER3D (*43*).

excitation wavelengths. The first wavelength allows one to analyze the contribution of both the 10 Tyr and the 2 Trp residues present in *Ss*EF-1α, whose location in the structure of *Ss*EF-1α·GDP is shown in Figure 3. The second wavelength induces the selective excitation of Trp residues. The fluorescence emission spectra of *Ss*EF-1α·GDP (Figure 4) upon excitation at 280 nm show a maximum at 308 nm, whereas those carried out upon excitation at 295 nm present a peak at 327 nm. Very similar spectra have been obtained for nf*Ss*EF-1α. The maximum at 308 nm should represent the contribution of Tyr residues, whereas the absence of a maximum for the two Trp residues could be the consequence of their quenching and/or the absence of resonance energy transfer between excited Tyr phenol rings and Trp side chains. The spectra obtained upon excitation at 295 nm present a maximum at 327 nm and a shoulder at 345−355 nm. This may indicate that the two Trp side chains are located in different environments. This result is in line with the structural data available on *Ss*EF-1α·GDP, indicating that Trp 209 is well-buried, whereas Trp 334 is partially exposed to the solvent (*15*). Because no difference is detectable

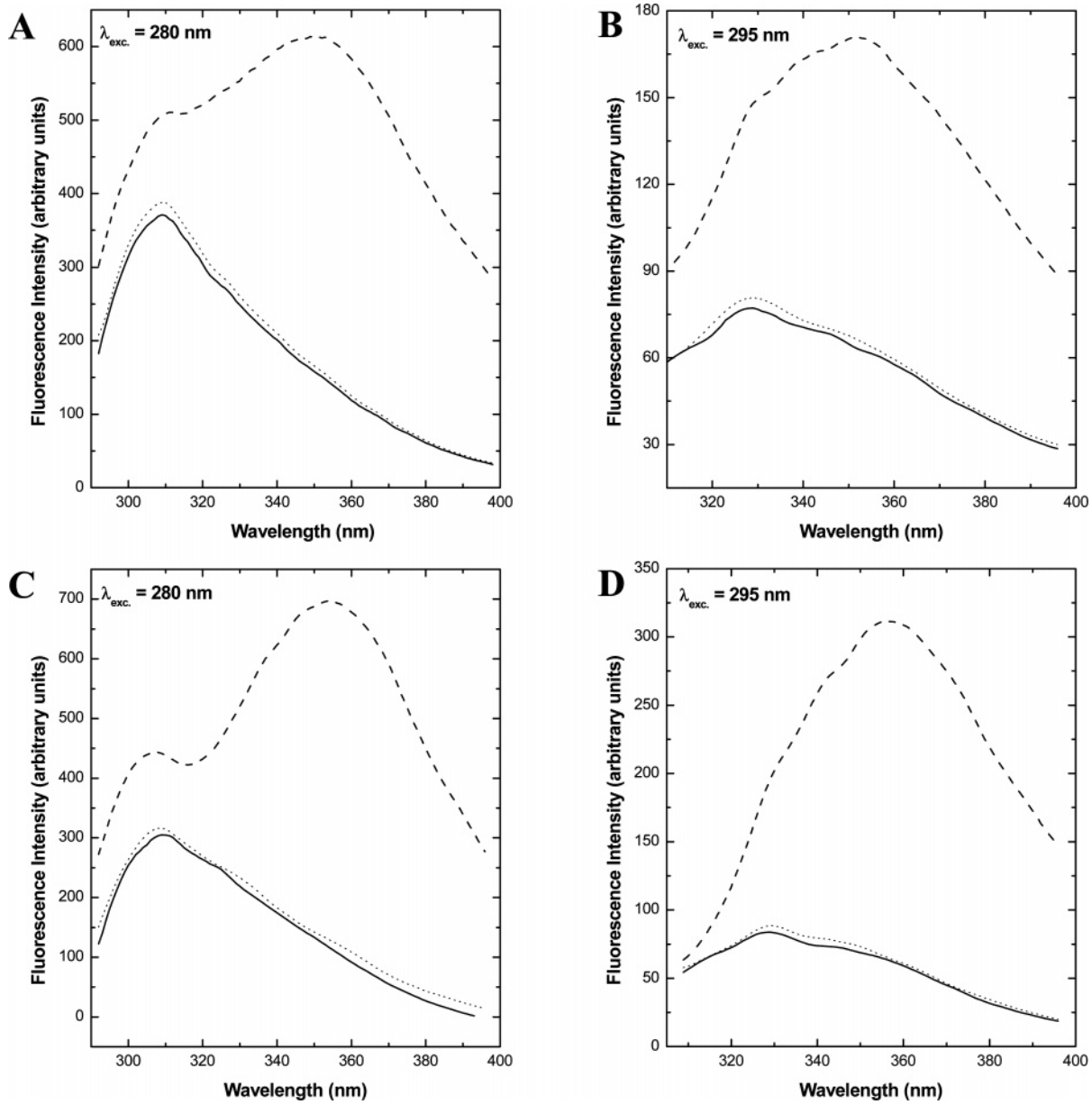

FIGURE 4: Fluorescence emission spectra of native (—), denatured (- - -), and renatured (•••) *Ss*EF-1α·GDP. Denaturation experiments were performed by using either 9.6 M urea (A and B) or 7.0 M GuHCl (C and D). Renaturation was achieved by removing the denaturing agent. In A and C, the excitation wavelength was 280 nm, whereas it was 295 nm for the experiments reported in B and D.

between the fluorescence spectra of *Ss*EF-1α·GDP and nf*Ss*EF-1α, these data confirm that the aromatic side chains are embedded in similar environments in both forms.

Upon chemical denaturation with either 7.0 M GuHCl or 9.6 M urea, the fluorescence spectra of both *Ss*EF-1α·GDP and nf*Ss*EF-1α show an increase of the quantum yield and maxima shifted to longer wavelengths, specifically 355 nm for GuHCl and 350 nm for urea (Figure 4), regardless of the excitation wavelength used. It is worth mentioning that fluorescence emission spectra with a maximum around 350 nm are characteristic of Trp side chains exposed to aqueous solvent (*24*). Therefore, both urea and GuHCl cause the destruction of the tertiary structure of *Ss*EF-1α. Moreover, the fluorescence emission spectra upon excitation at 280 nm of both protein forms, either in 9.6 M urea or 7.0 M GuHCl, show a second lower maximum at 310 nm because of the emission of Tyr side chains (see parts A and C in Figure 4). The occurrence of this peak is an indication that the resonance energy transfer from Tyr side chains to Trp ones is not complete in denatured *Ss*EF-1α.

Finally, it is worth noting that the unfolding of *Ss*EF-1α·GDP by chemical denaturants also produces the dissociation of GDP from the enzyme. The removal of both denaturant and GDP by dialysis leads to the formation of the folded nucleotide-free form of *Ss*EF-1α, because the denaturation process is reversible (see below). Therefore, this procedure represents an alternative method to obtain nf*Ss*EF-1α.

Stability against Chemical Denaturants. The conformational stability of nf*Ss*EF-1α and *Ss*EF-1α·GDP against the denaturing action of both urea and GuHCl was investigated by recording as a function of the denaturant concentration: the change in molar ellipticity at 222 nm and the change in fluorescence intensity at 308 (upon excitation at 280 nm) and at 327 nm (upon excitation at 295 nm) (Figure 5). The experiments were carried out at 20 °C, in a 10 mM phosphate buffer (pH 7.0), after an overnight incubation of the samples

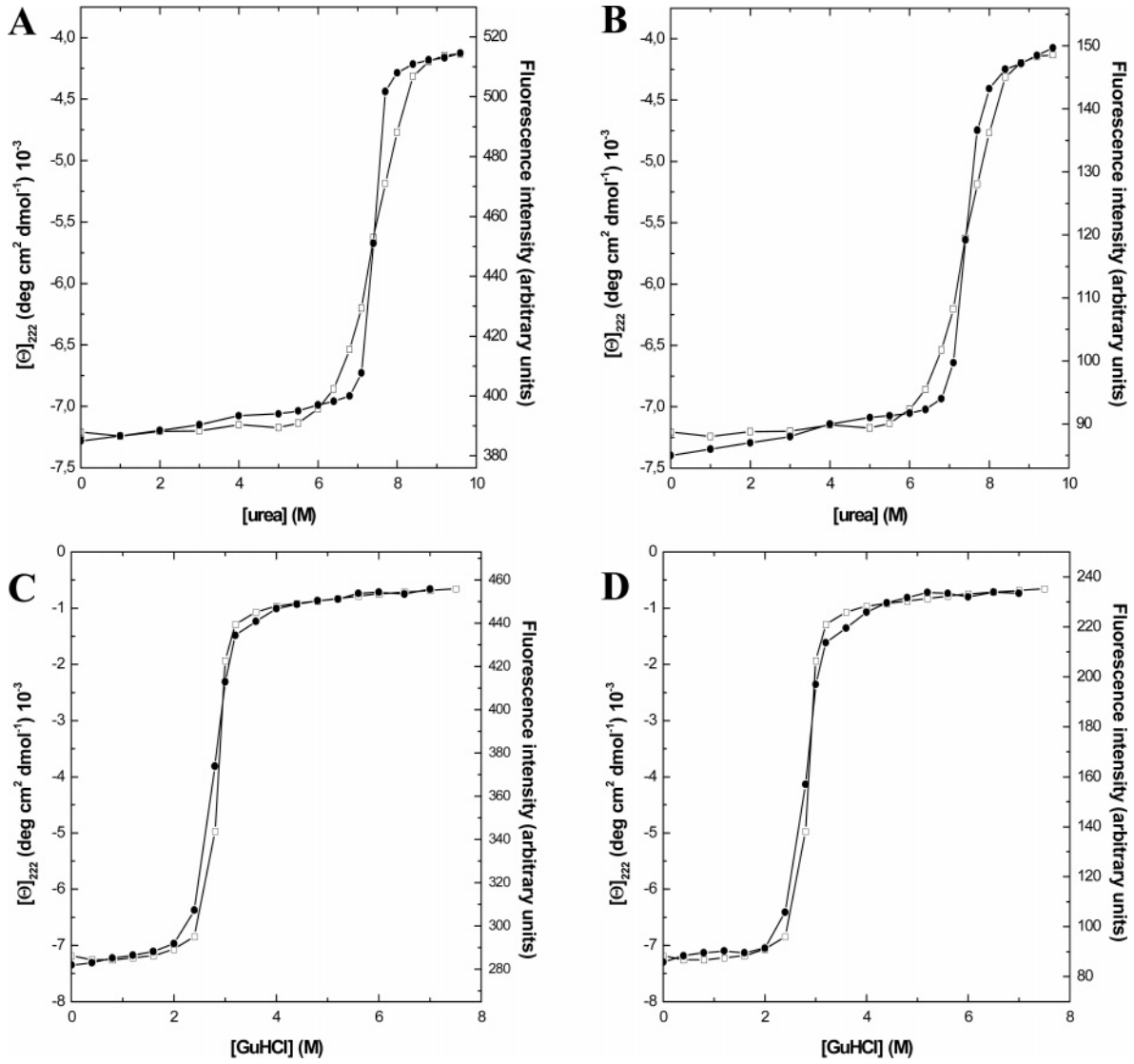

FIGURE 5: Equilibrium denaturation curves of *Ss*EF-1α·GDP induced at pH 7.0 and 20 °C by urea (A and B) or GuHCl (C and D). The curves were obtained by recording the change of the fluorescence intensity (I_{nat}) at 308 and 327 nm (●) and the change of the molar ellipticity at 222 nm (□). The curves of the change of the fluorescence intensity reported in A and C were obtained upon excitation at 280 nm, whereas those shown in B and D were recorded upon excitation at 295 nm. The protein concentration was 0.15 mg mL^{-1}.

at 4 °C. The results proved to be independent of the protein concentration in the range of 0.05−0.4 mg mL^{-1}.

Renaturation of completely unfolded samples upon suitable dilutions showed a full recovery of all of the spectroscopic features of the native enzyme (Figures 1 and 4). The reversibility of the unfolding process of *Ss*EF-1α·GDP induced by GuHCl was confirmed by recording the change of the molar ellipticity at 222 nm upon dilution of a protein solution containing 5 M GuHCl (Figure 6). Similar results were obtained when the change of the fluorescence intensity was used as a probe (data not shown). Analogous findings are obtained for nf*Ss*EF-1α (data not shown).

It is worth mentioning that, upon dilution, GuHCl-unfolded samples exhibit an intrinsic GTPase activity (see Figure S1 in the Supporting Information) and a GDP-binding ability (Figure S2 in the Supporting Information) that are similar to those shown by wild-type *Ss*EF-1α (*16*).

The denaturation curves obtained by means of the independent experimental probes show similar features for both *Ss*EF-1α·GDP and nf*Ss*EF-1α. They have a sigmoidal shape with a single inflection point, typical of a cooperative phenomenon. Similar inflection points are observed when the shift of the wavelength of the maximum of the fluorescence spectra is considered. Furthermore, the values of the denaturant concentration at half-completion of the transition, $[urea]_{1/2}$ (7.2−7.4 M) and $[GuHCl]_{1/2}$ (2.7−2.9 M), are virtually independent of the experimental probe used (see Table 1).

DISCUSSION

The structure of *Ss*EF-1α is characterized by the presence of three distinct domains, which constitute a widespread supradomain motif found in several other systems (*25*). The domain organization of the protein complexed with GDP is peculiar. Upon analogy with the complexes of EF-Tu·GDP, *Ss*EF-1α·GDP presents a triangular shape with a large hole located between domains 1 and 2 (Figure 3). The atypical shape of the protein structure and the unusual living conditions of the host organism prompted us to investigate the stability against chemical denaturants of *Ss*EF-1α·GDP and nf*Ss*EF-1α.

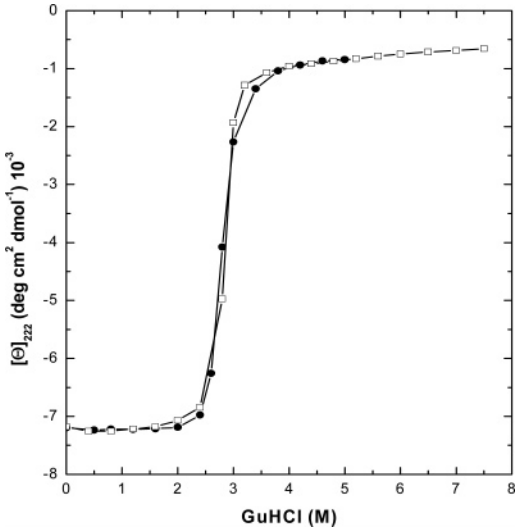

FIGURE 6: Reversibility of the unfolding process of *Ss*EF-1α·GDP induced by GuHCl. The curves were obtained by recording the change of the molar ellipticity at 222 nm of protein solutions treated overnight with increasing amounts of GuHCl (□) or upon dilution of a protein solution containing 5 M GuHCl (●).

Table 1: Values of the Denaturant Concentration at Half-Completion of the Transition for *Ss*EF-1α·GDP[a]

	probe	$[urea]_{1/2}$	$[GuHCl]_{1/2}$
$\lambda_{exc} = 280$ nm	$[\theta]_{222}$	7.4 (7.4)	2.9 (2.9)
	I_{nat}[b]	7.4 (7.4)	2.8 (2.8)
	λ_{max}	7.4 (7.2)	2.8 (2.8)
$\lambda_{exc} = 295$ nm	I_{nat}[b]	7.4 (7.4)	2.8 (2.7)
	λ_{max}	7.4 (7.3)	2.8 (2.7)

[a] The values for nfSsEF-1α are reported in parenthesis. The numbers are the mean values of these measurements; the estimated errors are approximately within 15% of the values reported. [b] I_{nat} corresponds to the fluorescence intensity at 308 and 327 nm for measurements carried out with λ_{exc} of 280 and 295 nm, respectively.

Upon excitation at 280 nm of both nf*Ss*EF-1α and *Ss*EF-1α·GDP, the fluorescence emission spectra are characterized by the presence of a peak at 308 nm because of Tyr emission. This unusual feature (*24*) is likely related to the peculiar structure of the protein. Indeed, the absence of detectable resonance energy transfer between tyrosine and tryptophan residues may be ascribed to the presence of four Tyr side chains, namely, Tyr 84, Tyr 180, Tyr 241, and Tyr 401, which have the center of mass located more than 20 Å away from the center of mass of both Trp side chains. Furthermore, the fluorescence intensity of the two Trp residues may be quenched because Trp 334 is partially exposed to the solvent and Trp 209 has the indole nitrogen atom involved in a hydrogen bond.

Notwithstanding the features of fluorescence spectra, the experimental data on the stability of both *Ss*EF-1α·GDP and nf*Ss*EF-1α against urea and GuHCl demonstrate unequivocally that the denaturant-induced unfolding is a cooperative and reversible process, which is accompanied by a total recovery of the enzymatic activity. Different probes, far-UV CD, and fluorescence, detecting changes in the secondary and tertiary structure, respectively, produce very similar transition curves with a single inflection point located at the same value of the denaturant concentration. These data indicate that the process can be described as a two-state N ⟺ D transition (*26*). This may appear surprising, given the

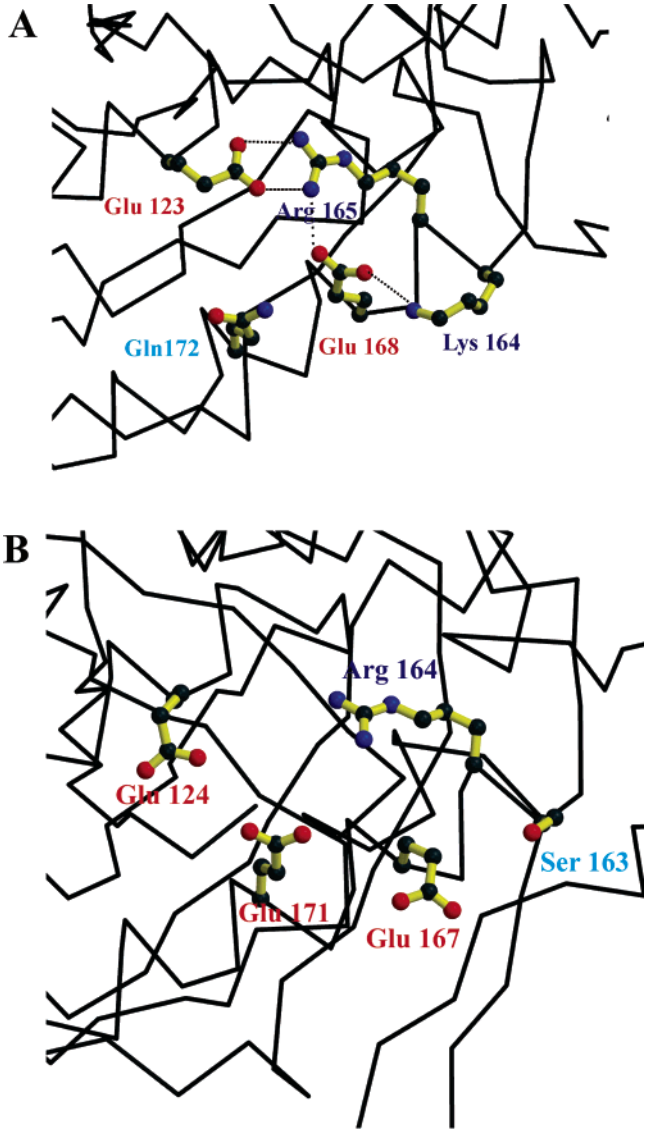

FIGURE 7: Cluster of charged residues in the structure of *Ss*EF-1α·GDP (*15*) (A). The corresponding residues in the structure of *Sc*EF-1α (*13*) are shown in B. Electrostatic interactions between atoms whose distance is shorter than 3.2 Å are shown with dashed lines.

dimensions and the shape of the protein. It is typically believed that the maximum size for a cooperative domain is about 200 residues (*27*−*29*). However, in recent years, several exceptions, especially among extremophilic proteins, have been found (*27*−*32*). The data presented here suggest that even a large protein with a rather loose structure can exhibit a cooperative unfolding. This finding also indicates that the structural alterations of a single domain can be transmitted to the others, despite the limited interdomain interfaces of the protein. Both *Ss*EF-1α forms exhibit a remarkable stability against urea, $[urea]_{1/2} = 7.2-7.4$ M. On the other hand, the stability against GuHCl is not particularly high, $[GuHCl]_{1/2} = 2.7-2.9$ M. This means that, even though *Ss*EF-1α comes from a hyperthermophilic source, it does not possess extra-resistance to the denaturing action of GuHCl. As found for other thermostable proteins, the ratio $[urea]_{1/2}/[GuHCl]_{1/2} \approx 2.8$ is significantly higher than that (approximately 2) obtained from analyses carried out on proteins isolated from mesophilic organisms (*33*, *34*). The relatively low $[GuHCl]_{1/2}$ value, compared to the $[urea]_{1/2}$

one, may indicate that electrostatic interactions, which are more efficiently weakened by GuHCl than urea, play an important role in the stabilization of *Ss*EF-1α.

This finding prompted us to carry out a survey of the electrostatic interactions that may play an important role in the stabilization of *Ss*EF-1α. The structure of *Sc*EF-1α (*13*) isolated from the mesophilic organism *S. cerevisiae*, was used as a reference. The analysis of the crystal structure of *Ss*EF-1α·GDP (*15*) reveals two important electrostatic clusters. The first one involves the side chains of Glu 216 and Arg 30, which belong to the helices A and F, respectively, of domain 1. Helix A is further stabilized by electrostatic interactions between Arg 25 and Asp 29 side chains. These residues are not conserved in the *Sc*EF-1α sequence. It is worth mentioning that Glu 216 is close to the 12-residue deletion/insertion region that differentiates EF-1α sequences of animals and fungi from those of plants, protists, and archaea (*35*).

The second cluster of electrostatic interactions involves the Arg 165 side chain, which interacts with both Glu 123 and Glu 168 (Figure 7A). The Glu168 side chain also interacts with the Lys 164 side chain. Interestingly, although the arginine and the two glutamic acid residues are conserved in the *S. cerevisiae* sequence, these electrostatic interactions are not optimized in the *Sc*EF-1α structure (Figure 7B), because of (a) the replacement of the lysine with a neutral residue, Ser 163, and (b) the presence of an additional negatively charged residue, Glu 171, in this region (Figure 7B). This shows how the formation of an ion pair strongly depends upon the local environment of the residues involved. Even though these electrostatic clusters, in line with a general survey (*36*), may represent important candidates for conferring stability to the *Ss*EF-1α, medium- and long-range interactions on the protein surface may also have stabilizing effects, as suggested in other cases (*37*−*41*). Along this line, it is worth mentioning that *Ss*EF-1α contains a slightly higher percentage (28 versus 26%) of charged residues (Lys, Arg, Glu, and Asp) and a lower amount (15 versus 17%) of polar residues (Asn, Ser, Gln, and Thr) when compared to *Sc*EF-1α.

ACKNOWLEDGMENT

We thank Dr. F. Catanzano for her contribution to the early stages of this work and G. Sorrentino, M. Amendola, and L. de Luca for their skillful technical assistance.

NOTE ADDED AFTER ASAP PUBLICATION

In an earlier version of this paper posted ASAP on the web on December 24, 2005, Glu 172 was incorrectly cited on line 352 in the last paragraph of the paper. This residue has been corrected to Glu 171 in this new version posted December 29, 2005.

SUPPORTING INFORMATION AVAILABLE

Figure S1, GTPase activity of native (△) and renatured GuHCl-unfolded *Ss*EF-1 (○) in the presence of 0.5 M NaCl; Figure S2, GDP-binding ability of native (A) and renatured GuHCl unfolded SsEF-1 (B). This material is available free of charge via the Internet at http://pubs.acs.org.

REFERENCES

1. Andersen, G. R., Nissen, P., and Nyborg, J. (2003) Elongation factors in protein biosynthesis, *Trends Biochem. Sci. 28*, 434−441.
2. Merrick, W. C., and Nyborg, J. (2000) The protein biosynthesis elongation cycle, in *Translational Control of Gene Expression* (Sonenberg, N., Hershey, J. W. B., and Mathews, M. B., Eds.) Cold Spring Harbor Laboratory Press, New York.
3. Abel, K., and Jurnak, F. (1996) A complex profile of protein elongation: Translating chemical energy into molecular movement, *Structure 4*, 229−238.
4. Kjeldgaard, M., Nyborg, J., and Clark, B. F. (1996) The GTP binding motif: Variations on a theme, *FASEB J. 10*, 1347−1368.
5. Berchtold, H., Reshetnikova, L., Reiser, C. O., Schirmer, N. K., Sprinzl, M., and Hilgenfeld, R. (1993) Crystal structure of active elongation factor Tu reveals major domain rearrangements, *Nature 365*, 126−132.
6. Kjeldgaard, M., Nissen, P., Thirup, S., and Nyborg, J. (1993) The crystal structure of elongation factor EF-Tu from *Thermus aquaticus* in the GTP conformation, *Structure 1*, 35−50.
7. Amils, R., Cammarano, P., and Londei, P. (1993) Translation in archaea, in *The Biochemistry of Archaea* (Kates, M., Kushner, D. J., and Matheson, A. T., Eds.) pp 393−438, Elsevier Science Publishers, Amsterdam, The Netherlands.
8. Kjeldgaard, M., and Nyborg, J. (1992) Refined structure of elongation factor EF-Tu from *Escherichia coli*, *J. Mol. Biol. 223*, 721−742.
9. Nissen, P., Kjeldgaard, M., Thirup, S., Polekhina, G., Reshetnikova, L., Clark, B. F., and Nyborg, J. (1995) Crystal structure of the ternary complex of Phe-tRNAPhe, EF-Tu, and a GTP analog, *Science 270*, 1464−1472.
10. Vogeley, L., Palm, G. J., Mesters, J. R., and Hilgenfeld, R. (2001) Conformational change of elongation factor Tu (EF-Tu) induced by antibiotic binding. Crystal structure of the complex between EF-Tu·GDP and aurodox, *J. Biol. Chem. 276*, 17149−17155.
11. Kawashima, T., Berthet-Colominas, C., Wulff, M., Cusack, S., and Leberman, R. (1996) The structure of the *Escherichia coli* EF-Tu·EF-Ts complex at 2.5 Å resolution, *Nature 379*, 511−518.
12. Wang, Y., Jiang, Y., Meyering-Voss, M., Sprinzl, M., and Sigler, P. B. (1997) Crystal structure of the EF-Tu·EF-Ts complex from *Thermus thermophilus*, *Nat. Struct. Biol. 4*, 650−656.
13. Andersen, G. R., Pedersen, L., Valente, L., Chatterjee, I., Kinzy, T. G., Kjeldgaard, M., and Nyborg, J. (2000) Structural basis for nucleotide exchange and competition with tRNA in the yeast elongation factor complex eEF1A:eEF1Bα, *Mol. Cell. 6*, 1261−1266.
14. Andersen, G. R., Valente, L., Pedersen, L., Kinzy, T. G., and Nyborg, J. (2001) Crystal structures of nucleotide exchange intermediates in the eEF1A−eEF1Bα complex, *Nat. Struct. Biol. 8*, 531−534.
15. Vitagliano, L., Masullo, M., Sica, F., Zagari, A., and Bocchini, V. (2001) The crystal structure of *Sulfolobus solfataricus* elongation factor 1α in complex with GDP reveals novel features in nucleotide binding and exchange, *EMBO J. 20*, 5305−5311.
16. Masullo, M., De Vendittis, E., and Bocchini, V. (1994) Archaebacterial elongation factor 1α carries the catalytic site for GTP hydrolysis, *J. Biol. Chem. 269*, 20376−20379.
17. Ianniciello, G., Masullo, M., Gallo, M., Arcari, P., and Bocchini, V. (1996) Expression in *Escherichia coli* of thermostable elongation factor 1α from the archaeon *Sulfolobus solfataricus*, *Biotechnol. Appl. Biochem. 23*, 41−45.
18. Raimo, G., Masullo, M., and Bocchini, V. (1999) The interaction between the archaeal elongation factor 1α and its nucleotide exchange factor 1*β*, *FEBS Lett. 451*, 109−112.
19. John, J., Sohmen, R., Feuerstein, J., Linke, R., Wittinghofer, A., and Goody, R. S. (1990) Kinetics of interaction of nucleotides with nucleotide-free H-ras p21, *Biochemistry 29*, 6058−6065.
20. Sreerama, N., and Woody, R. W. (1993) A self-consistent method for the analysis of protein secondary structure from circular dichroism, *Anal. Biochem. 209*, 32−44.
21. Lobley, A., Whitmore, L., and Wallace, B. A. (2002) DICHROWEB: An interactive website for the analysis of protein secondary structure from circular dichroism spectra, *Bioinformatics 18*, 211−212.
22. Vitagliano, L., Ruggiero, A., Masullo, M., Cantiello, P., Arcari, P., and Zagari, A. (2004) The crystal structure of *Sulfolobus solfataricus* elongation factor 1α in complex with magnesium and GDP, *Biochemistry 43*, 6630−6636.
23. Tanfani, F., Scire, A., Masullo, M., Raimo, G., Bertoli, E., and Bocchini, V. (2001) Salts induce structural changes in elongation factor 1α from the hyperthermophilic archaeon *Sulfolobus solfataricus*: A Fourier transform infrared spectroscopic study, *Biochemistry 40*, 13143−13148.

24. Lakowicz, J., R, (1999) *Principles of Fluorescence Spectroscopy*, Kluwer Academic and Plenum Publishers, New York.
25. Chothia, C., Gough, J., Vogel, C., and Teichmann, S. A. (2003) Evolution of the protein repertoire, *Science 300*, 1701−1703.
26. Cantor, C. R., and Schimmel, P. R. (1980) *Biophysical Chemistry*, W. H. Freeman and Company, New York.
27. Spassov, V. Z., Karshikoff, A. D., and Ladenstein, R. (1995) The optimization of protein−solvent interactions: Thermostability and the role of hydrophobic and electrostatic interactions, *Protein Sci. 4*, 1516−1527.
28. Privalov, P. L. (1989) Thermodynamic problems of protein structure, *Annu. Rev. Biophys. Biophys. Chem. 18*, 47−69.
29. Dill, K. A. (1985) Theory for the folding and stability of globular proteins, *Biochemistry 24*, 1501−1509.
30. del Vecchio, P., Graziano, G., Granata, V., Barone, G., Mandrich, L., Rossi, M., and Manco, G. (2002) Denaturing action of urea and guanidine hydrochloride towards two thermophilic esterases, *Biochem. J. 367*, 857−863.
31. del Vecchio, P., Graziano, G., Granata, V., Farias, T., Barone, G., Mandrich, L., Rossi, M., and Manco, G. (2004) Denaturant-induced unfolding of the acetyl-esterase from *Escherichia coli*, *Biochemistry 43*, 14637−14643.
32. Feller, G., d'Amico, D., and Gerday, C. (1999) Thermodynamic stability of a cold-active α-amylase from the Antarctic bacterium Alteromonas haloplanctis, *Biochemistry 38*, 4613−4619.
33. Myers, J. K., Pace, C. N., and Scholtz, J. M. (1995) Denaturant *m* values and heat capacity changes: Relation to changes in accessible surface areas of protein unfolding, *Protein Sci. 4*, 2138−2148.
34. Dempsey, C. E., Piggot, T. J., and Mason, P. E. (2005) Dissecting contributions to the denaturant sensitivities of proteins, *Biochemistry 44*, 775−781.
35. Baldauf, S. L., and Palmer, J. D. (1993) Animals and fungi are each other's closest relatives: Congruent evidence from multiple proteins, *Proc. Natl. Acad. Sci. U.S.A. 90*, 11558−11562.
36. Karshikoff, A., and Ladenstein, R. (2001) Ion pairs and the thermotolerance of proteins from hyperthermophiles: A "traffic rule" for hot roads, *Trends Biochem. Sci. 26*, 550−556.
37. Cambillau, C., and Claverie, J. M. (2000) Structural and genomic correlates of hyperthermostability, *J. Biol. Chem. 275*, 32383−32386.
38. Makhatadze, G. I., Loladze, V. V., Gribenko, A. V., and Lopez, M. M. (2004) Mechanism of thermostabilization in a designed cold shock protein with optimized surface electrostatic interactions, *J. Mol. Biol. 336*, 929−942.
39. Sanchez-Ruiz, J. M., and Makhatadze, G. I. (2001) To charge or not to charge? *Trends Biotechnol. 19*, 132−135.
40. Pace, C. N. (2000) Single surface stabilizer, *Nat. Struct. Biol. 7*, 345−346.
41. Suhre, K., and Claverie, J. M. (2003) Genomic correlates of hyperthermostability, an update, *J. Biol. Chem. 278*, 17198−17202.
42. Kraulis, P. J. (1991) MOLSCRIPT: A program to produce both detailed and schematic plots of protein structures, *J. Appl. Crystallogr. 24*, 946−950.
43. Merritt, E. A., and Bacon, D. J. (1997) Raster3D: Photorealistic molecular graphics, *Methods Enzymol. 277*, 505−524.

BI050479D